



Fast color balance and multi-path fusion for sandstorm image enhancement

Bo Wang¹ · Bowen Wei¹ · Zitong Kang¹ · Li Hu¹ · Chongyi Li²

Received: 5 June 2020 / Revised: 15 August 2020 / Accepted: 14 September 2020
© Springer-Verlag London Ltd., part of Springer Nature 2020

Abstract

Outdoor images captured during sandstorm weather condition frequently yield color cast and poor visibility, which causes some applications to fail in computer vision, such as video surveillance and object recognition systems. In this paper, a fast color balance method followed by an effective fusion model is proposed to enhance the sandstorm-degraded images. Firstly, color channel compensation and piece-wise affine transform balance the aberrant pixels obtained by camera and remove color cast. Then, multi-path fusion comprising of underexposure and contrast-enhanced inputs is used for visibility enhancement, where saturation and Laplacian contrast are measured as weight maps and constructed for Gaussian pyramids. In order to reduce block effects and artifacts of the reconstructed image, we introduce the multi-scale strategy for each path. Experimental results of both synthetic and real-world sandstorm images demonstrate that the proposed color balance method features high computational efficiency and performs much better than comparative methods in terms of image quality. In addition, our fusion-based method also outperforms existing enhancement algorithms of sandstorm image via qualitative and quantitative evaluations.

Keywords Sandstorm image · Color balance · Multi-path fusion · Weight maps

1 Introduction

Poor visibility of images caused by inclement weather condition seriously influences the performance of outdoor object recognition, video surveillance systems, remote sensing systems and so on. In particular, compared with hazy images, sandstorm images exhibit undesirable color shift effects, very low contrast and visibility due to floating sand-dust particles absorbing and scattering the incident light to the lens of cameras. Therefore, the large absorption of blue hue of the spectrum by atmospheric particles results in characteristic distributions of RGB color histograms, which makes the sandstorm images show brown, yellow or even orange in different situations.

Intuitively, color constancy-based methods can be implemented to correct poor illumination and color-biased images, thus restoring color information of objects and scenes. There are a number of classic and computationally efficient approaches used for estimating the color of the light source and achieving color constancy, i.e., Grey-World (GW) [1], Max-RGB (MRGB) [2], Shades-of-Grey (SoG) [3], Grey-Edge (GE) [4], Weighted Grey-Edge (Weighted-GE) [5]. On the other hand, in order to enhance visibility of hazy images, many studies have focused on methods called dehazing. Dark channel prior (DCP) or multi-scale fusion-based methods have been widely applied for haze removal, thereby obtaining higher contrast and better visibility [6–8]. Whereas it is a fact that the radius and opacity of floating particles under sandstorm environment are substantially larger than that under mist or fog weather, different priors are no longer applicable to current situation suffering from severe color cast and naturalness distortion.

Recently, some algorithms that specifically enhance sandstorm images have been attracting much attention due to its significance in computer vision tasks. Fu et al. [9] developed a strategy based on color correction and image fusion. There were two inputs with different brightness deriving from the

✉ Bo Wang
tjuwb@nxu.edu.cn

¹ School of Physics and Electronic-Electrical Engineering, Ningxia University, Yinchuan 750021, People's Republic of China

² School of Computer Science and Engineering, Nanyang Technological University, Singapore 639798, Singapore

color-corrected image by gamma correction. Although this classic approach obtained good results on several real-world images, it was still limited on degraded scenes with severe color distortion and drastic luminance changes. Huang et al. [10, 11] proposed a depth estimation and color analysis-based method for visibility restoration of sandstorm images. However, it was mainly developed from DCP that may overcorrect the color in bright area and make the corresponding results show blue shift. In [12], Yu et al. initially estimated atmospheric light based on the scattering model and the GW assumption, and the transmission map was estimated using information loss constraint. While the resulting images were improved in terms of visibility, the overall color looked unnatural due to GW color-corrected method. Zhi et al. [13] adopted normal distribution model for color cast removal and singular value decomposition for details enhancement. Pan et al. [14] used Gaussian model to adjust color and information loss constraints combined with DCP to enhance contrast. Whereas the visibility of large depth region based on the above two methods was still poor according to the results. In [15], Shi et al. presented a method using halo-reduced DCP dehazing and achieved good visibility on a number of sandstorm images. But the color cast cannot be effectively removed based on general GW assumption in LAB color space.

In this paper, we propose a color channel compensation and piece-wise affine transform-based method that could not only remove color cast but also have the advantage of computational efficiency. According to color characteristics of sandstorm image that large absorption of blue hue by atmospheric particles, we employ combined channel with red and green to compensate for blue channel attenuation. After blue channel compensation, the scale of each color channel will be stretched under an assumption that the lowest values of R, G, B must correspond to black and the highest values of that must correspond to white [16]. Therefore, the color cast can be further removed and higher contrast of image can be obtained with implementation of the affine transform. Next, multi-scale fusion for different path including underexposure and contrast-enhanced is proposed to obviously improve visibility, i.e., more details and natural appearance are shown in the final fused image.

The rest of this paper is organized as follows. Section 2 provides details of the proposed method of sandstorm image enhancement. In Sect. 3, some experimental results and analysis are reported. Finally, conclusion and future work are presented in Sect. 4.

2 Color balance and multi-path fusion

The flowchart of our proposed sandstorm image enhancement method is illustrated in Fig. 1, which is primarily

comprised of two steps. To begin with, the color balance is conducted to correct color distortion of the degraded sandstorm images instead of resorting to any traditional white balance strategy. Then, the improved multi-scale fusion is performed with multi-path inputs including underexposure and contrast-enhanced images, which makes details of the region with high-intensity clearer and higher local contrast of the region with middle and small depth in a scene. Finally, the results of the multi-path are combined linearly, which takes good advantage of both their merit.

2.1 Fast color balance

When focusing on visibility enhancement of sandstorm images, we need to balance the aberrant pixels. The sandstorm images generally look brown, yellow or even orange, which exhibit different histogram distributions. However, the concentrated distribution of each color channel must be arranged in descending order from R to B according to observation of a large number of sandstorm images, which can be seen from the corresponding RGB histogram in Fig. 2.

According to the display order, light with shorter wavelength, i.e., the blue light, is commonly lost more when traveling in the air, followed by green light. Therefore, we resort to adding a term of combination with red and green channel as opponent information to compensate blue attenuation at each pixel location as follow:

$$I_{BC}(x) = I_B(x) + \alpha((\bar{I}_R + \bar{I}_G)/2 - \bar{I}_B) \times (1 - I_B(x))((I_R(x) + I_G(x))/2) \quad (1)$$

where \bar{I}_R , \bar{I}_G and \bar{I}_B represent the mean value of the red I_R , green I_G and blue I_B channel, respectively.

Since the red channel involves opponent color information compared to the green channel [17], we simultaneously employ a fraction of the red channel to compensate the green one when it is seriously attenuated and only blue compensation is obviously inadequate:

$$I_{GC}(x) = I_G(x) + \alpha(\bar{I}_R - \bar{I}_G)(1 - I_G(x))I_R(x) \quad (2)$$

where α is set to 1.0 for different illumination conditions and each channel for compensation is normalized to interval [0, 1].

After color compensation, the sandstorm images still have poor contrast and color cast due to the distribution of pixels in each channel keeping relatively concentrated pattern. Given that each color channel of an input image is reshaped as an array of M numeric values between [0, 255], and each channel is processed independently, our proposed piece-wise affine transform can map different intervals into appropriate ranges. The corresponding output of each channel can be regarded as a contrast and color-corrected array of M updated numeric

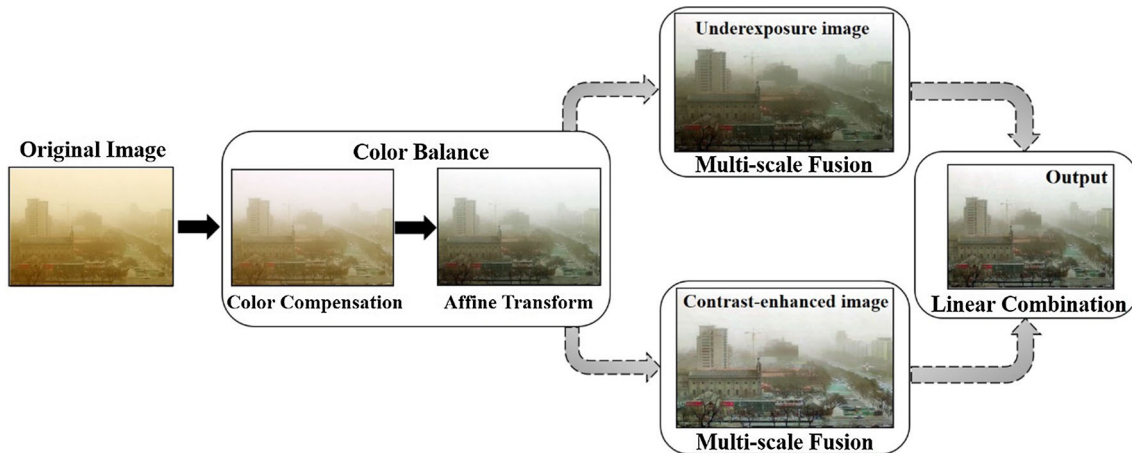


Fig. 1 The flowchart of the proposed method

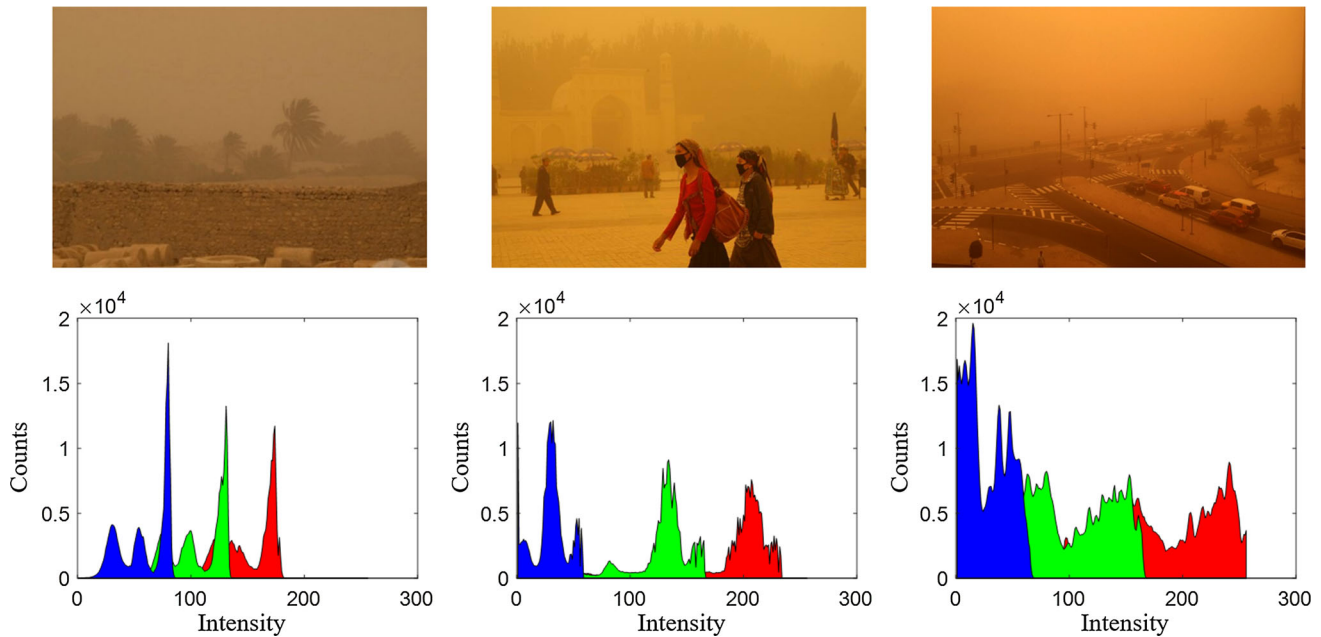


Fig. 2 Typical RGB histogram of sandstorm images

values. There are 5 sub-intervals are defined according to the distribution characteristic of pixels after color compensation and the possible ranges are $[0, V_{\min-1}]$, $[V_{\min-1}, V_{\min}]$, $[V_{\min}, V_{\max}]$, $[V_{\max}, V_{\max+1}]$ and $[V_{\max+1}, 255]$, respectively, where \min denotes the value of the $(p\% \times M)$ th pixel and \max denotes the value of the $((1-p\%) \times M + 1)$ th pixel, p is set to be 0.1. The piece-wise linear transform is illustrated as Fig. 3.

2.2 Multi-path fusion

After color balance that is crucial to restore the genuine color, dehazing problem has to be considered in next step since the details of the scene need to be further unveiled.

Compared with those traditional dehazing methods based on optical model, our method does not require estimation of the transmission map and atmospheric light that are not easy to be precisely calculated. Therefore, in this paper, we propose a multi-scale fusion strategy based on multi-path sandstorm image inputs for dehazing. There are two groups of input images that have been removed color cast and their corresponding weight maps derived from each scale. Different inputs originate from underexposed and contrast-limited adaptive histogram equalization (CLAHE) processing [18], respectively, which is illustrated in Fig. 4.

Underexposure inputs are generated to unveil more details of region that has pixels with brighter intensities. Whereas the region with darker intensities that are usually closer to

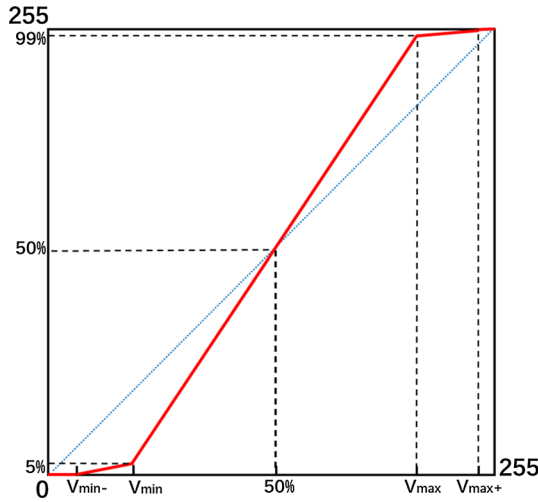


Fig. 3 Piece-wise linear transform

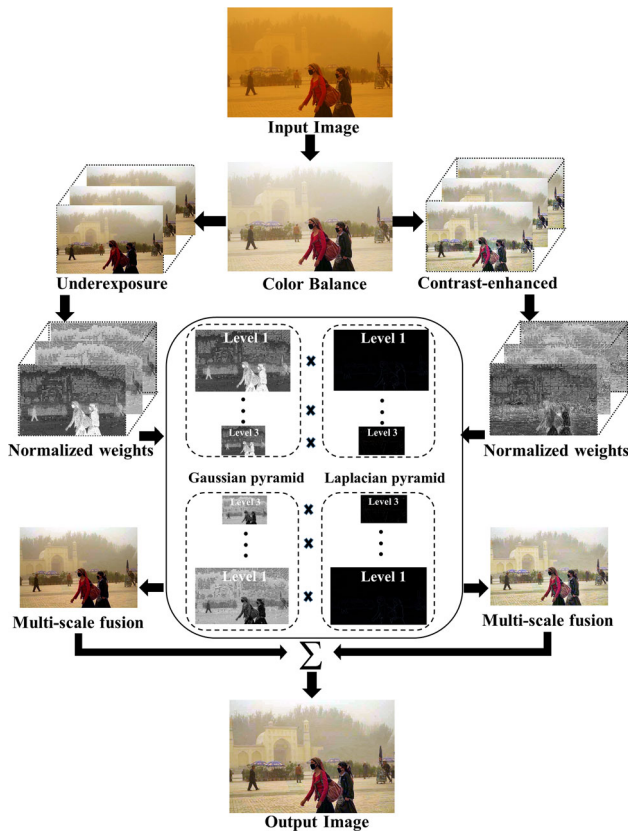


Fig. 4 Overview of multi-path fusion

camera cannot be correctly exposed at the same time, thereby possibly produces too dark regions with very low contrast. Accordingly, the other path including inputs that enhance local contrast of the image is introduced as compensation for this loss and meanwhile obviously alters the visibility of large scene depth. Besides, contrast and saturation at each pixel is measured as weight maps that are used to preserve

the local image quality, that is, higher value of weight maps will be more represented in fused image.

Specifically, gamma correction as an intuitive method is employed to control exposure of image, which can be implemented by a power-function transform:

$$T(\bar{I}) = \bar{I}^\gamma \quad (3)$$

In this paper, correction of underexposure ($\gamma > 1$) is presented for visibility enhancement of middle and far range depth of the scene, which is more seriously affected by scattering and absorption problem. Inspired by [19], multiple exposed image fusion can be regarded as an effective method to show more details of various regions. Thus, a series of images can be obtained by power-function transform using different gamma values. After preprocessing of sandstorm image, hazy area that is comprised of pixels with brighter intensities can be more easily distinguished due to expansive dynamic range. In order to compensate the originally well-exposed areas, CLAHE processing is introduced into another path. Then, the result of multi-scale fusion from this path can be capable of depicting more details due to local histogram equalization and finally create the fused output image that achieves the correct exposure.

In each path, the optimal weight maps are fused with a set of inputs at each pixel (x, y) for reconstructed image $O(x, y)$, which can be defined as follows:

$$O_u(x, y) = \sum_{k=1}^K \bar{W}_k^u(x, y) \bar{I}_k^u(x, y) \quad (4)$$

$$O_c(x, y) = \sum_{k=1}^K \bar{W}_k^c(x, y) \bar{I}_k^c(x, y) \quad (5)$$

where \bar{I}_k^u and \bar{I}_k^c represent input images using underexposure and CLAHE processing, respectively, \bar{W}_k^u and \bar{W}_k^c denote normalized weight maps, k indicates the index of each input and $K = 3$, the exposed and clip-range step is set to be 0.2 and 0.04 for underexposure and CLAHE in this paper.

As for metrics used for local image quality, e.g. Laplacian contrast and saturation, they can be measured for weights and defined as follows:

$$C_k(x, y) = \frac{\partial^2 \bar{I}_k}{\partial x^2}(x, y) + \frac{\partial^2 \bar{I}_k}{\partial y^2}(x, y) \quad (6)$$

$$S_k(x, y) = \sum_{i \in \{R, G, B\}} \left(\bar{I}_k^i(x, y) - \frac{\bar{I}_k^R(x, y) + \bar{I}_k^G(x, y) + \bar{I}_k^B(x, y)}{3} \right)^2 \quad (7)$$

As a result, the final weights can be obtained by $\bar{W}_k(x, y) = C_k(x, y) \times S_k(x, y)$. In order to avoid obvious halos or artifacts, multi-scale method is adopted in this part.

Let F_G^n to denote a sequence of low-pass filters and down-sampling followed by n up-sampling operations, N levels F_L^n of the pyramid can be defined as:

$$\begin{aligned}\bar{I}(x, y) &= \bar{I}(x, y) - F_G^1\{\bar{I}(x, y)\} + F_G^1\{\bar{I}(x, y)\} \\ &\triangleq F_L^1\{\bar{I}(x, y)\} + F_G^1\{\bar{I}(x, y)\} \\ &= F_L^1\{\bar{I}(x, y)\} + F_G^1\{\bar{I}(x, y)\} \\ &\quad - F_G^2\{\bar{I}(x, y)\} + F_G^2\{\bar{I}(x, y)\} \\ &= F_L^1\{\bar{I}(x, y)\} + F_L^2\{\bar{I}(x, y)\} + F_G^2\{\bar{I}(x, y)\} \\ &= \dots \\ &= \sum_{n=1}^N F_L^n\{\bar{I}(x, y)\}\end{aligned}\quad (8)$$

$$O_u^n(x, y) = \sum_{k=1}^K F_G^n\{\bar{W}_k^u(x, y)\} F_L^n\{\bar{I}_k^u(x, y)\} \quad (9)$$

$$O_c^n(x, y) = \sum_{k=1}^K F_G^n\{\bar{W}_k^c(x, y)\} F_L^n\{\bar{I}_k^c(x, y)\} \quad (10)$$

$$O_U(x, y) = \sum_{n=1}^N O_u^n(x, y) \uparrow^d \quad (11)$$

$$O_C(x, y) = \sum_{n=1}^N O_c^n(x, y) \uparrow^d \quad (12)$$

$$O_f(x, y) = \omega_G O_U(x, y) + \omega_C O_C(x, y) \quad (13)$$

The input image $\bar{I}_k(x, y)$ is decomposed by a Laplacian pyramid, and each normalized weight map \bar{W}_k is decomposed by a Gaussian pyramid. Accordingly, the Laplacian inputs and the Gaussian normalized weights can be fused at each level n , where \uparrow^d signifies up-sampling operator making it twice as its size. Finally, the output $O_f(x, y)$ will be linearly fused with $O_U(x, y)$ and $O_C(x, y)$, where ω_G and ω_C are set to be 0.5 and 0.5.

3 Experiments and analysis

In order to verify the validity of the proposed method, we first test performance of color balance on synthesized image for qualitative and quantitative comparison. The original testing image is chosen from Dolls category in Middlebury 2005 dataset, and we set 50% as the percentage of opacity to simulate sandstorm image. PSNR (Peak Signal to Noise Ratio), SSIM (Structural Similarity Index), FSIM (Feature Similarity Index) and FSIMc [20] are employed to quantitatively evaluate the performance of the proposed color balance

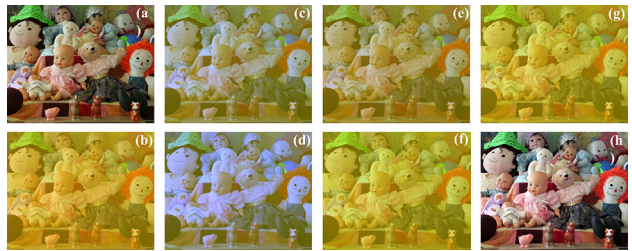


Fig. 5 The qualitative comparison on synthetic image

Table 1 The evaluation on synthetic image in terms of PSNR, SSIM, FSIM and FSIMc

Method	PSNR (dB)	SSIM	FSIM	FSIMc
SoG	16.2543	0.8038	0.8925	0.8577
GW	13.4863	0.7106	0.9013	0.8493
MRGB	15.8939	0.8034	0.8780	0.8431
GE	12.9271	0.7242	0.8907	0.8384
Weighted-GE	12.8680	0.7223	0.8900	0.8377
Proposed	19.0556	0.9176	0.9763	0.9680

method, and the higher PSNR and SSIM values indicate less noise and better similarity with original image. Moreover, processing speed of color balance is also compared with classic white-balancing methods. Then, we conduct experiments on 40 real-world sandstorm images and compare the results with 3 typical methods (i.e., Fu et al. [9], Al-Ameen [21], Shi et al. [15]) using image quality assessment (IQA). All the experiments are implemented on Matlab2018a with Intel i7-7500U CPU, 8.00 GB RAM. The parameters of our method are set as described in Sect. 2.

3.1 Evaluation of fast color balance

An example of qualitative comparison on synthetic image (i.e., Fig. 5b) is shown in Fig. 5. Figure 5c–h presents the results of white-balancing techniques, i.e., SoG, GW, MRGB, GE, Weighted-GE and our proposed method, respectively. As can be seen from Fig. 5, the classic white-balancing methods are failure to remove the color cast. Compared with white-balancing methods, the proposed approach can obtain better consistency with the original image (i.e., Fig. 5a) in terms of genuine color and good visibility. Table 1 shows the quantitative results of different methods based on PSNR and SSIM metrics. The results demonstrate the superiority of our proposed color balance method and are consistent with the visual effect in Fig. 5.



Fig. 6 The qualitative comparison on real-world image

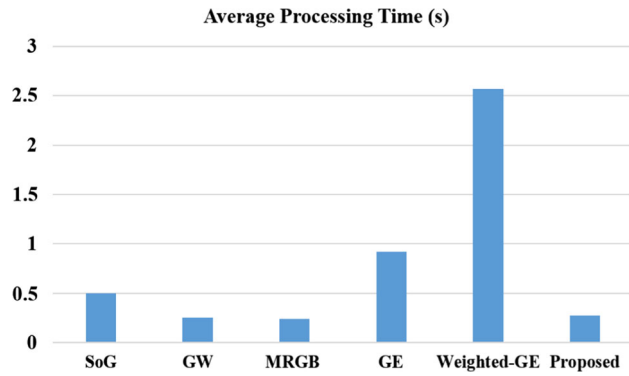


Fig. 7 The average processing time of dataset

According to the comprehensive assessment, as mentioned in Table 1 and Fig. 5, Weighted-GE method will be excluded for experiment on typical real-world image. Figure 6b-f shows the results of GW, SoG, MRGB, GE and our proposed method, respectively. As can be seen from Fig. 6, the result of our proposed method (Fig. 6f) can effectively remove color cast of image captured in severe polluted dust weather and obtain better contrast as well.

Next, we test the processing speed of color-balancing method on a sandstorm image dataset comprised of 40 images with various resolution. The average processing time of dataset is illustrated in Fig. 7. Our proposed approach shows remarkable computational efficiency. Figure 8 illustrates the running times for various image sizes via GW and our fast approach. We can see that the running time of both methods significantly increases when the image size becomes larger than 2.8 M pixels.

3.2 Evaluation of multi-path fusion

To further evaluate the effectiveness of multi-path fusion, we make subjective and objective comparisons with 3 sandstorm image enhancement methods. Several typical sandstorm images including urban transportation, people and buildings are chosen from the dataset. As shown in Fig. 9, all the methods can effectively remove color cast except for the Al-Ameen's results. Fu et al.'s method obtains color balance, but

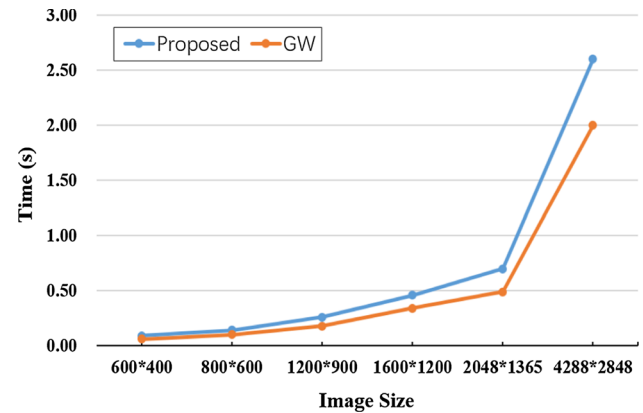


Fig. 8 Running time of GW and the proposed method

Table 2 The image quality assessment of results

Method	Entropy	IVM	CG	NIQE
Fu et al.'s	6.8662	4.3298	0.1031	3.9245
Al-Ameen's	6.4125	4.9948	0.1190	3.7548
Shi et al.'s	7.0708	5.6004	0.1693	3.6232
Proposed	7.6974	5.1185	0.2177	3.5048

is still not satisfactory in terms of the brightness, contrast and color saturation. In contrast, the results of Shi et al.'s method achieve better brightness, while remains haze effect leading to worse visual quality.

According to the results from Fig. 9, our proposed method outperforms comparative methods in terms of visibility, brightness and contrast, which can be simultaneously verified with objective image quality assessment (i.e., entropy, NIQE [22], IVM and CG [23] and) shown in Table 2. It should be noted that larger image entropy, IVM and CG indicate more contained useful information, visible edge and contrast gain while lower values represent better image quality when using NIQE. The best performance is highlighted in bold.

4 Conclusion and future work

In this paper, we have presented an effective method for sandstorm image enhancement. Our fast color-balancing method is able to obtain genuine color while preserve more similar image structure and achieve higher PSNR. Multi-path fusion combines advantage of different outputs and does not require any additional information. According to the results based on a real-world dataset we have collected, both subjective and objective comparisons reveal superiority of our proposed method. In future work, we will extend the dataset toward more challenging sandstorm images and videos.

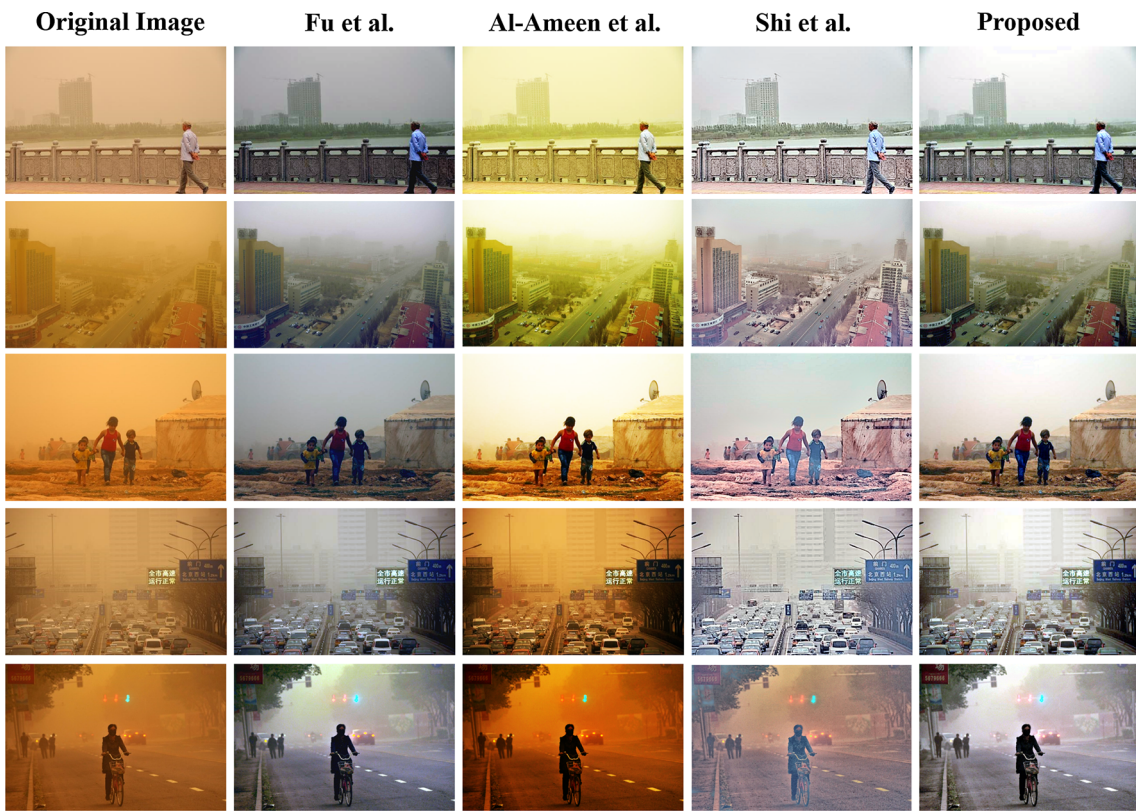


Fig. 9 Subjective comparisons on typical sandstorm images from dataset

Acknowledgements This work is supported by Higher Education Scientific Research Project of Ningxia (NGY2017009).

Funding This work is supported by Higher Education Scientific Research Project of Ningxia (NGY2017009).

Availability of data and material The raw data can be shared if the researchers need to do research on relevant topic and cite it in their papers.

Code availability The code can be shared in the near future for the sake of development.

Compliance with ethical standards

Conflict of interest No conflict of interest exists in the submission of this manuscript, and the manuscript is approved by all authors for publication.

References

1. Gijsenij, A., Gevers, T., Van De Weijer, J.: Computational color constancy: survey and experiments. *IEEE Trans. Image Process.* **20**(9), 2475–2489 (2011)
2. Land, E.: The retinex theory of colour vision. *Sci. Am.* **237**(6), 108–128 (1977)
3. Finlayson, G.D., Trezzi, E.: Shades of gray and colour constancy. In: *Proceedings of Color and Imaging Conference*, pp. 37–41 (2004)
4. Van De Weijer, J., Gevers, T., Gijsenij, A.: Edge-based color constancy. *IEEE Trans. Image Process.* **16**(9), 2207–2214 (2007)
5. Gijsenij, A., Gevers, T., Van De Weijer, J.: Improving color constancy by photometric edge weighting. *IEEE Trans. Pattern Anal. Mach. Intell.* **34**(5), 918–929 (2012)
6. He, K., Sun, J., Tang, X.: Single image haze removal using dark channel prior. *IEEE Trans. Pattern Anal. Mach. Intell.* **33**(12), 2341–2353 (2011)
7. Zhao, D., Xu, L., Yan, Y., Chen, J., Duan, L.: Multi-scale optimal fusion model for single image dehazing. *Signal Process. Image Commun.* **74**, 253–265 (2019)
8. Li, Y., Miao, Q., Liu, R., Song, J., Quan, Y., Huang, Y.: A multi-scale fusion scheme based on haze-relevant features for single image dehazing. *Neurocomputing* **283**, 73–86 (2018)
9. Fu, X., Huang, Y., Zeng, D., Zhang, X.P., Ding, X.: A fusion-based enhancing approach for single sandstorm image. In: *2014 IEEE 16th International Workshop on Multimedia Signal Processing*, pp. 1–5. IEEE, Jakarta (2014)
10. Huang, S., Chen, B., Wang, W.: Visibility restoration of single hazy images captured in real-world weather conditions. *IEEE Trans. Circ. Syst. Video Technol.* **24**(10), 1814–1824 (2014)
11. Huang, S., Ye, J., Chen, B.: An advanced single-image visibility restoration algorithm for real-world hazy scenes. *IEEE Trans. Ind. Electron.* **62**(5), 2962–2972 (2014)
12. Yu, S., Zhu, H., Wang, J., Fu, Z., Xue, S., Shi, H.: Single sand-dust image restoration using information loss constraint. *J. Mod. Opt.* **63**(21), 2121–2130 (2016)

13. Zhi, N., Mao, S., Li, M.: Visibility restoration algorithm of dust-degraded images. *J. Image Graph.* **21**(12), 1585–1592 (2016)
14. Pan, H., Tian, R., Liu, C., Gong, C.: A sand-dust degraded image enhancement algorithm based on color correction and information loss constraints. *J. Comput. Aided Des. Comput. Graph.* **30**(6), 992–999 (2018)
15. Shi, Z., Feng, Y., Zhao, M., Zhang, E., He, L.: Let you see in sand dust weather: a method based on halo-reduced dark channel prior dehazing for sand-dust image enhancement. *IEEE Access* **7**, 116722–116733 (2019)
16. Morel, J.M., Petro, A.B., Sbert, C.: Screened Poisson equation for image contrast enhancement. *Image Process. On Line* **4**, 16–29 (2014)
17. Ancuti, C.O., Ancuti, C., De Vleeschouwer, C., Bekaert, P.: Color balance and fusion for underwater image enhancement. *IEEE Trans. Image Process.* **27**(1), 379–393 (2017)
18. Zuiderveld, K., Heckbert, P.: Contrast limited adaptive histogram equalization. In: *Graphics Gems IV*. New York (1994)
19. Galdran, A.: Image dehazing by artificial multiple-exposure image fusion. *Signal Process.* **149**, 135–147 (2018)
20. Zhang, L., Zhang, L., Mou, X., Zhang, D.: FSIM: a feature similarity index for image quality assessment. *IEEE Trans. Image Process.* **20**(8), 2378–2386 (2011)
21. Al-Ameen, Z.: Visibility enhancement for images captured in dusty weather via tuned tri-threshold fuzzy intensification operators. *Int. J. Intell. Syst. Appl.* **8**(8), 10–17 (2016)
22. Mittal, A., Soundararajan, R., Bovik, A.C.: Making a “completely blind” image quality analyzer. *IEEE Signal Process. Lett.* **20**(3), 209–212 (2013)
23. Xu, Y., Wen, J., Fei, L., Zhang, Z.: Review of video and image defogging algorithms and related studies on image restoration and enhancement. *IEEE Access* **4**, 165–188 (2016)

Publisher's Note Springer Nature remains neutral with regard to jurisdictional claims in published maps and institutional affiliations.